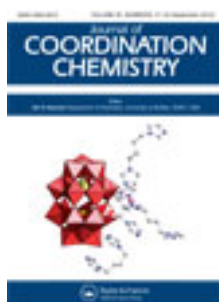


This article was downloaded by: [Renmin University of China]

On: 13 October 2013, At: 10:37

Publisher: Taylor & Francis

Informa Ltd Registered in England and Wales Registered Number: 1072954 Registered office: Mortimer House, 37-41 Mortimer Street, London W1T 3JH, UK



Journal of Coordination Chemistry

Publication details, including instructions for authors and subscription information:

<http://www.tandfonline.com/loi/gcoo20>

A new nickel(II) complex with the thiosemicarbazone of quinoline-2-carboxaldehyde: structure, DNA-binding, cleavage, and cytotoxic activities

Shouchun Zhang^a, Juanjuan Dong^a, Xiaorui Fan^a, Yun Chen^b & Jianliang Zhou^a

^a School of Chemistry and Chemical Engineering, Central South University, Changsha 410083, P.R. China

^b School of Chemistry and Chemical Engineering, Hunan University, Changsha 410082, P.R. China

Accepted author version posted online: 10 Jul 2012. Published online: 24 Jul 2012.

To cite this article: Shouchun Zhang, Juanjuan Dong, Xiaorui Fan, Yun Chen & Jianliang Zhou (2012) A new nickel(II) complex with the thiosemicarbazone of quinoline-2-carboxaldehyde: structure, DNA-binding, cleavage, and cytotoxic activities, Journal of Coordination Chemistry, 65:17, 3098-3110, DOI: [10.1080/00958972.2012.710842](https://doi.org/10.1080/00958972.2012.710842)

To link to this article: <http://dx.doi.org/10.1080/00958972.2012.710842>

PLEASE SCROLL DOWN FOR ARTICLE

Taylor & Francis makes every effort to ensure the accuracy of all the information (the "Content") contained in the publications on our platform. However, Taylor & Francis, our agents, and our licensors make no representations or warranties whatsoever as to the accuracy, completeness, or suitability for any purpose of the Content. Any opinions and views expressed in this publication are the opinions and views of the authors, and are not the views of or endorsed by Taylor & Francis. The accuracy of the Content should not be relied upon and should be independently verified with primary sources of information. Taylor and Francis shall not be liable for any losses, actions, claims, proceedings, demands, costs, expenses, damages, and other liabilities whatsoever or howsoever caused arising directly or indirectly in connection with, in relation to or arising out of the use of the Content.

This article may be used for research, teaching, and private study purposes. Any substantial or systematic reproduction, redistribution, reselling, loan, sub-licensing, systematic supply, or distribution in any form to anyone is expressly forbidden. Terms & Conditions of access and use can be found at <http://www.tandfonline.com/page/terms-and-conditions>

A new nickel(II) complex with the thiosemicarbazone of quinoline-2-carboxaldehyde: structure, DNA-binding, cleavage, and cytotoxic activities

SHOUCHUN ZHANG*†, JUANJUAN DONG†, XIAORUI FAN†,
YUN CHEN‡ and JIANLIANG ZHOU†

†School of Chemistry and Chemical Engineering,
Central South University, Changsha 410083, P.R. China

‡School of Chemistry and Chemical Engineering, Hunan University,
Changsha 410082, P.R. China

(Received 22 February 2012; in final form 6 June 2012)

[Ni(QTS)₂]·Cl·CH₃OH, where QST = quinoline-2-carboxaldehyde thiosemicarbazone, has been synthesized and characterized. The complex crystallized in a monoclinic system with space group *P*2(1)/*n*. Nickel(II) is situated in a distorted octahedral geometry with two tridentate ligands and one ligand is mono-deprotonated to coordinate to nickel(II). Interaction of the nickel(II) complex with calf thymus DNA was investigated by electronic absorption, CD, and fluorescence spectra. The results suggest that nickel(II) complex binds to DNA through a groove binding mode. The nickel(II) complex exhibited efficient DNA cleavage at micromolar concentration in the presence of ascorbate with hydroxyl radicals as the active species. *In vitro* cytotoxicity assay showed that the nickel(II) complex was more potent against MCF-7 cell line but less active against A-549 cell line than cisplatin at the concentrations tested.

Keywords: Nickel complex; Thiosemicarbazone; DNA-binding; DNA cleavage; Cytotoxicity

1. Introduction

Thiosemicarbazones and their derivatives with wide pharmacological versatility, such as anticancer, antibacterial, antiviral, antifungal, and antimicrobial activities, have received attention [1–6]. These compounds have excellent capacity to coordinate with many transition metal ions, and the generated complexes show significant biological activities [7–13]. In many cases, the activities of these complexes are higher than that of the thiosemicarbazone alone [14–17].

Many studies suggest that thiosemicarbazones and derivatives with biological activities usually have a nitrogen-containing heterocycle (e.g., α -pyridyl moiety) adjacent to the N¹ position [18–22]. For example, 2-formylpyridine thiosemicarbazone reported about 50 years again was the first α -(*N*)-heterocyclic carboxaldehyde thiosemicarbazone with antitumor properties [23]. Later, 5-hydroxy-2-formylpyridine

*Corresponding author. Email: zhang_shch@yahoo.com.cn

thiosemicarbazone was developed as the first compound of this series that entered phase I clinical trials. However, the high instability and severe side effects prevented its further clinical development [24, 25]. Another representative example was 3-aminopyridine-2-carboxaldehyde thiosemicarbazone, which entered clinical trials for the treatment of a variety of malignancies [26–28]. Many other α -pyridylthiosemicarbazones and their metal complexes with promising biological activities have been investigated [29–32].

We focus our research on the synthesis and antitumor activities of new α -(*N*)-heterocyclic carboxaldehyde thiosemicarbazones and their metal complexes to find more potent pharmacological agents. It is commonly thought that DNA is the primary pharmacological target of many antitumor compounds, and interaction between metal complexes and DNA is in close relationship with their potential biological and pharmaceutical activities [33–35]. Binding modes to DNA would give insights into the biochemical mechanism of action of the complexes, which have been of interest for development of effective chemotherapeutic agents.

Here we report the synthesis and characterization of a new nickel(II) complex with thiosemicarbazone of quinoline-2-carboxaldehyde. The DNA-binding, DNA cleavage and *in vitro* cytotoxic activities of the nickel(II) complex are also studied.

2. Experimental

2.1. Chemicals and physical measurements

Common reagents such as $\text{NiCl}_2 \cdot 6\text{H}_2\text{O}$, thiosemicarbazide, ethanol, methanol, and anhydrous ether are of analytical grade and used as received. Plasmid pBR322 and disodium salt of calf thymus DNA (CT-DNA) were commercially available from MBI Fermentas, while quinoline-2-carboxaldehyde, ascorbate, tris(hydroxy-methyl) amino-methane (Tris), and ethidium bromide (EB) were from Sigma. Infrared spectra were recorded on a Bruker VECTOR22 spectrometer as KBr pellets ($4000\text{--}500\text{ cm}^{-1}$) and elemental analysis was performed on a Perkin-Elmer 240°C analytical instrument. UV-Vis spectra were recorded on a UV-3100 spectrometer. CD spectra were obtained by using a Jasco J-810 automatic recording spectropolarimeter. Fluorescence spectra were recorded on an AMINCO Bowman Series 2 Luminescence Spectrometer.

2.2. Synthesis

2.2.1. Ligand. Quinoline-2-carboxaldehyde thiosemicarbazone (QTS) was obtained following a similar procedure reported [30] by condensation of thiosemicarbazide and quinoline-2-carboxaldehyde (1 : 1 ratio) in ethanol.

2.2.2. $[\text{Ni}(\text{QTS})_2] \cdot \text{Cl} \cdot \text{CH}_3\text{OH}$. A methanol solution (20 mL) of $\text{NiCl}_2 \cdot 6\text{H}_2\text{O}$ (0.5 mmol, 119 mg) was added dropwise to methanol solution (20 mL) of QTS (1 mmol, 230 mg), and the resulting solution was refluxed for 4 h. Dark red block single crystals suitable for X-ray diffraction were obtained on slow evaporation of the solution of the complex. IR/(KBr, ν/cm^{-1}): 3269, 3149 $\nu(\text{N-H})$, 1567 $\nu(\text{C=N})$, 1123 $\nu(\text{C=S})$. Anal. Calcd for $\text{C}_{23}\text{H}_{23}\text{N}_8\text{OS}_2\text{ClNi}$ (%): C, 47.16; H, 3.95; N, 19.12. Found (%): C, 47.08; H, 3.98; N, 19.19.

Table 1. Crystal data and structure refinement for $[\text{Ni}(\text{QTS})_2] \cdot \text{Cl} \cdot \text{CH}_3\text{OH}$.

Empirical formula	$\text{C}_{23}\text{H}_{23}\text{N}_8\text{NiS}_2\text{ClO}$
Formula weight	585.77
Temperature (K)	273(2)
Crystal system	Monoclinic
Space group	$P2(1)/n$
Unit cell dimensions (\AA , $^\circ$)	
a	10.7127(6)
b	9.5598(5)
c	24.2734(13)
α	90
β	94.748(2)
γ	90
Volume (\AA^3), Z	2477.3(2), 4
Calculated density (Mg m^{-3})	1.571
Absorption coefficient (mm^{-1})	1.095
$F(000)$	1208
θ range for data collection ($^\circ$)	2.15–28.00
Limiting indices	$-12 \leq h \leq 14$; $-12 \leq k \leq 11$; $-31 \leq l \leq 29$
Reflection collected/unique	17,318/5482 ($R_{\text{int}} = 0.1865$)
Absorption correction	Empirical
Refinement method	Full-matrix least-squares on F^2
Data/restraints/parameters	5482/1/327
Goodness-of-fit on F^2	0.983
Final R indices [$I > 2\sigma(I)$]	$R_1 = 0.0981$; $wR_2 = 0.2488$
R indices (all data) ^a	$R_1 = 0.2075$; $wR_2 = 0.3705$
Largest difference peak and hole (e \AA^{-3})	1.147 and -1.574

$$^a R_1 = \Sigma ||F_o| - |F_c|| / \Sigma |F_o|; wR_2 = [\Sigma w(F_o^2 - F_c^2)^2 / \Sigma w(F_o^2)^2]^{1/2}.$$

2.3. X-ray crystallography

Details of the crystal parameters, data collection, and refinement are listed in table 1. The structure was determined on a Siemens P4 four-circle diffractometer. Cell constants and an orientation matrix for data collection were obtained by least-squares refinement of diffraction data from 34 reflections in the range $1.84 < \theta < 24.97$. Data were collected at 293 K using monochromated Mo-K α radiation and the ω - 2θ scan technique with a variable scan speed of 5.0–50.0 min^{-1} in ω and corrected for Lorentz and polarization effects. An empirical absorption correction was made (ψ -scan). The structure was solved by Patterson methods and completed by iterative cycles of least-squares refinement and ΔF -syntheses. Hydrogen atoms were located in their calculated positions and treated as riding on the atoms to which they are attached. All non-hydrogen atoms were refined anisotropically. All calculations were carried out using SHELXTL [36].

2.4. Spectroscopic studies on DNA interaction

2.4.1. Electronic absorption spectra. The UV absorbances at 260 and 280 nm of CT-DNA solution in 50 mmol L^{-1} NaCl/5 mmol L^{-1} Tris-HCl buffer (pH 7.2) give a ratio of ~ 1.9 , indicating that the DNA was sufficiently free of protein [37]. The DNA concentration was determined by measuring the UV absorption at 260 nm, taking the

molar absorption coefficient (ϵ_{260}) of CT-DNA as $6600 \text{ (mol L}^{-1}\text{)}^{-1}\text{cm}^{-1}$ [38]. Electronic spectra of $[\text{Ni}(\text{QTS})_2] \cdot \text{Cl} \cdot \text{CH}_3\text{OH}$ ($5.0 \times 10^{-5} \text{ mol L}^{-1}$) were recorded before and after addition of CT-DNA ($r=0.0, 0.2, 0.4, 0.6, 0.8, 1.0, 1.2$, where r is the molar ratio of DNA and complex) in the 5 mmol L^{-1} Tris-HCl/ 50 mmol L^{-1} NaCl buffer. The intrinsic binding constant K_b for interaction of the studied complexes with CT-DNA was calculated by electronic absorption spectral titration data using the following equation [39]:

$$[\text{DNA}]/(\epsilon_a - \epsilon_f) = [\text{DNA}]/(\epsilon_b - \epsilon_f) + 1/K_b(\epsilon_b - \epsilon_f),$$

where ϵ_a , ϵ_f , and ϵ_b correspond to $A_{\text{obsd}}/[\text{Ni}]$, the extinction coefficient for the free nickel complex, and the extinction coefficient for the nickel(II) complex in the fully bound form, respectively. In the plot of $[\text{DNA}]/(\epsilon_a - \epsilon_f)$ versus $[\text{DNA}]$, K_b is then given by the ratio of the slope to intercept.

2.4.2. CD spectra. CD spectra of in the absence and presence of nickel(II) complex were collected. All CD experiments were carried out on a Jasco-810 spectropolarimeter at room temperature from 220 to 320 nm.

2.4.3. Fluorescence spectra. Fluorescence spectra were recorded at room temperature with excitation at 520 nm and emission at 600 nm. The experiment was carried out by titrating $[\text{Ni}(\text{QTS})_2] \cdot \text{Cl} \cdot \text{CH}_3\text{OH}$ ($5.0 \times 10^{-5} \text{ mol L}^{-1}$ in 5 mmol L^{-1} Tris-HCl/ 50 mmol L^{-1} NaCl buffer) into samples containing $1.0 \times 10^{-4} \text{ mol L}^{-1}$ DNA and $1.0 \times 10^{-5} \text{ mol L}^{-1}$ EB.

2.5. DNA cleavage

A typical reaction was carried out by mixing $1 \mu\text{L}$ of pBR322 DNA ($0.1 \mu\text{g}/\mu\text{L}$), $4.2 \mu\text{L}$ of Tris-HCl/NaCl buffer (pH 7.4) and $2.4 \mu\text{L}$ $[\text{Ni}(\text{QTS})_2] \cdot \text{Cl} \cdot \text{CH}_3\text{OH}$ solution in 40 mmol L^{-1} Tris-HCl/NaCl buffer (pH 7.4, 4% DMF) with $2.4 \mu\text{L}$ of ascorbate (H_2A) at a 50-fold molar excess relative to the complex to yield a total volume of $10 \mu\text{L}$. After mixing, the sample was incubated at 310 K for 1 h. The reactions were quenched by addition of ethylenediaminetetraacetic acid (EDTA) and loading buffer (0.25% bromphenol blue, 50% glycerol). Then, the solution was subjected to electrophoresis on 0.7% agarose gel in TBE buffer (89 mmol L^{-1} Tris, 89 mmol L^{-1} H_3BO_3 and 2 mmol L^{-1} EDTA) at 100 V and visualized by EB staining. The Gel Imaging and Documentation DigiDoc-ItTM System (Version 1.1.23, UVP, Inc. Unpland, CA) was assessed using Labworks Imaging and Analysis Software (UVP, Inc. Unpland, CA).

In the inhibition reactions, scavengers of reactive oxygen intermediates, DMSO, *tert*-butyl alcohol, and histidine ($2 \mu\text{L}$) were added initially to pBR322 DNA (100 ng) in the Tris-HCl/NaCl buffer and incubated for 15 min at 310 K prior to addition of $[\text{Ni}(\text{QTS})_2] \cdot \text{Cl} \cdot \text{CH}_3\text{OH}$ and H_2A . The mixture was diluted with the buffer to a total volume of $10 \mu\text{L}$. After a further incubation of 3 h at 310 K the sample was subjected to gel electrophoresis using the described procedures.

2.6. Cytotoxicity assay

The *in vitro* cytotoxicity of $[\text{Ni}(\text{QTS})_2] \cdot \text{Cl} \cdot \text{CH}_3\text{OH}$ was tested against the human breast cancer cell line MCF-7 by 3-(4,5-dimethylthiazole-2-yl)-2,5-diphenyltetrazolium bromide (MTT) assay [40] and against the human non-small-cell lung cancer cell line A-549 by sulforhodamine B (SRB) assay [41]. Cisplatin was chosen as a positive reference. The detailed procedure of the assay has been described in our previous work [42].

3. Results and discussion

3.1. Crystal structure

The molecular structure and atom-numbering schemes for $[\text{Ni}(\text{QTS})_2] \cdot \text{Cl} \cdot \text{CH}_3\text{OH}$ are shown in figure 1. Selected bond lengths and angles are summarized in table 2.

Nickel(II) is coordinated by two QST ligands in a distorted octahedral geometry through two *cis* quinolinyl nitrogen atoms (N(1) and N(5)) and two *cis* thiolato sulfurs (S(1) and S(2)) in the square plane, and two *trans* imine nitrogen atoms (N(2) and N(6)) in axial positions. Both QTS ligands are tridentate and the ligands show a (*Z*, *E*, *Z*)-configuration for these three donors, respectively. Similar meridional configurations of tridentate NNS ligands around nickel(II) have also been observed in other bischelated nickel(II) complexes of NNS thiosemicarbazones [43]. The C(22)–S(2) (1.690(8) Å) bond length is shorter than C(11)–S(1) (1.716(7) Å). Bond angles of N(6)–N(7)–C(22)

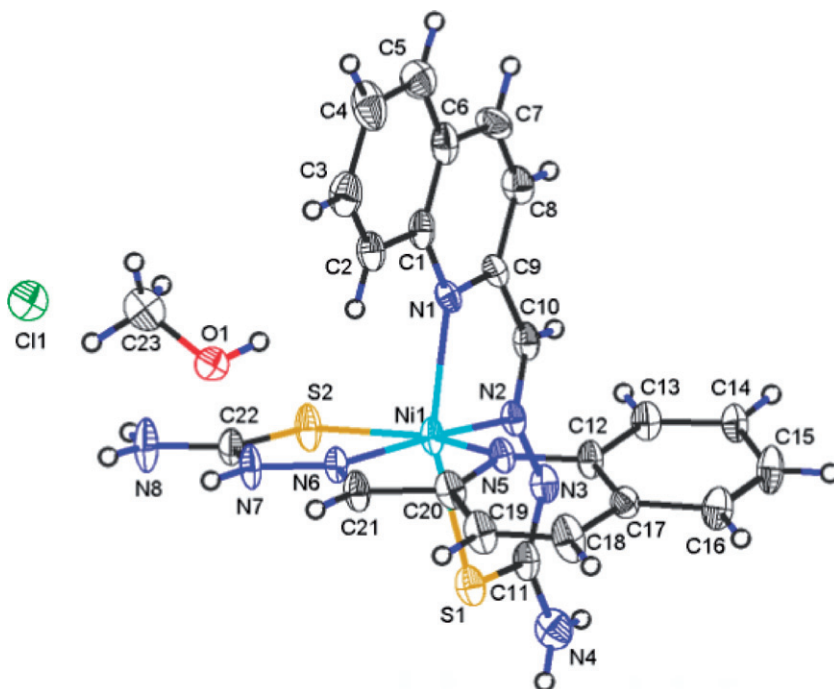


Figure 1. ORTEP diagram for $[\text{Ni}(\text{QTS})_2] \cdot \text{Cl} \cdot \text{CH}_3\text{OH}$.

Table 2. Selected bond lengths (Å) and angles (°) of [Ni(QTS)₂]·Cl·CH₃OH.

Ni(1)–N(1)	2.180(7)	Ni(1)–N(5)	2.175(6)	Ni(1)–S(1)	2.409(3)
Ni(1)–N(2)	2.024(6)	Ni(1)–N(6)	2.036(6)	Ni(1)–S(2)	2.429(2)
S(1)–C(11)	1.716(7)	S(2)–C(22)	1.690(8)		
N(1)–Ni(1)–N(2)	77.6(3)	N(2)–Ni(1)–N(6)	169.6(3)	N(1)–Ni(1)–S(2)	91.63(18)
N(1)–Ni(1)–N(5)	94.9(3)	N(1)–Ni(1)–S(1)	156.49(16)	N(2)–Ni(1)–S(2)	90.36(17)
N(1)–Ni(1)–N(6)	107.8(3)	N(2)–Ni(1)–S(1)	81.0(2)	N(5)–Ni(1)–S(2)	157.62(16)
N(5)–Ni(1)–N(6)	76.9(2)	N(5)–Ni(1)–S(1)	84.2(2)	N(6)–Ni(1)–S(2)	80.73(17)
N(2)–Ni(1)–N(5)	111.9(2)	N(6)–Ni(1)–S(1)	94.9(2)	S(1)–Ni(1)–S(2)	98.04(10)
N(2)–N(3)–C(11)	111.8(6)	N(6)–N(7)–C(22)	118.8(6)	S(1)–C(11)–N(3)	128.5(7)
S(2)–C(22)–N(7)	122.3(5)	S(1)–C(11)–N(4)	117.0(7)	S(2)–C(22)–N(8)	121.8(7)
	D–H (Å)	H···A (Å)	D···A (Å)	D–H···A (°)	
Hydrogen-bonding contacts D–H···A					
N(4)–H(4 A)···Cl(1) ⁱ	0.860	2.462	3.272	157.32	
N(4)–H(4B)···Cl(1) ⁱⁱ	0.860	2.558	3.345	152.52	
N(8)–H(8 A)···Cl(1) ⁱⁱⁱ	0.860	2.389	3.247	175.53	
N(8)–H(8B)···Cl(1)	0.860	2.887	3.573	138.00	

ⁱ= $x-1, y, z$; ⁱⁱ= $-x+1/2, y-1/2, -z+1/2$; ⁱⁱⁱ= $-x+2/3, y-1/2, -z+1/2$.

(118.8(6)°) and N(8)–C(22)–S(2) (121.8(7)°) are bigger than that of N(2)–N(3)–C(11) (111.8(6)°) and N(4)–C(11)–S(1) (117.0(7)°), while the N(7)–C(22)–S(2) bond angle (122.3(5)°) is smaller than that of N(3)–C(11)–S(1) (128.5(7)°). These bond lengths and angles show excellent agreement with those proposed by García-Tojal *et al.* to distinguish neutral or anionic form in ligands based on pyridine-2-carbaldehyde thiosemicarbazone [44] and ratify the coexistence of both forms of QTS in the same nickel(II) complex. Chloride is a counterion in this complex. The Ni–S [2.409(3) and 2.429(2) Å], Ni–N_{imine} [2.024(6) and 2.036(6) Å], and Ni–N_{quinoline} [2.180(7) and 2.175(6) Å] bond lengths are similar to those of other six-coordinate distorted octahedral nickel(II) complexes of tridentate sulfur–nitrogen chelating agents [45, 46]. The two Ni–N_{quinoline} bond lengths are very close and longer than Ni–N_{imine} bond lengths, indicative of weak coordination by quinoline. The bond angles of N(1)–Ni(1)–S(1) (156.49(16)°) and N(5)–Ni(1)–S(2) (157.62(16)°) are contracted from the ideal value of 180° for a regular square-planar structure, and the bond angle of N(2)–Ni(1)–N(6) (169.6(3)°) is also contracted from 180°, suggesting distorted octahedral geometry. Several hydrogen-bonding interactions are established in the lattice. The most relevant are given in table 2.

3.2. Spectral studies of the interactions with DNA

3.2.1. Electronic absorption spectra. It is very common to apply electronic absorption spectroscopy in DNA-binding studies [47]. Electronic absorption spectra of [Ni(QTS)₂]·Cl·CH₃OH in the absence and presence of CT-DNA are shown in figure 2. The bands at 238 and 293 nm can be assigned to $\pi \rightarrow \pi^*$ transitions of the coordinated thiosemicarbazone. Band at 339 nm and weak shoulder around 350 nm can be attributed to $n \rightarrow \pi^*$ transitions of the coordinated thiosemicarbazone. Bands at 383 and 423 nm must be due to L \rightarrow M transfer from sulfur to nickel. Occurrence of S \rightarrow M (LMCT) bands is quite common in electronic spectra of metal complexes of thiosemicarbazones [48, 49]. Upon increasing the concentration of DNA, moderate

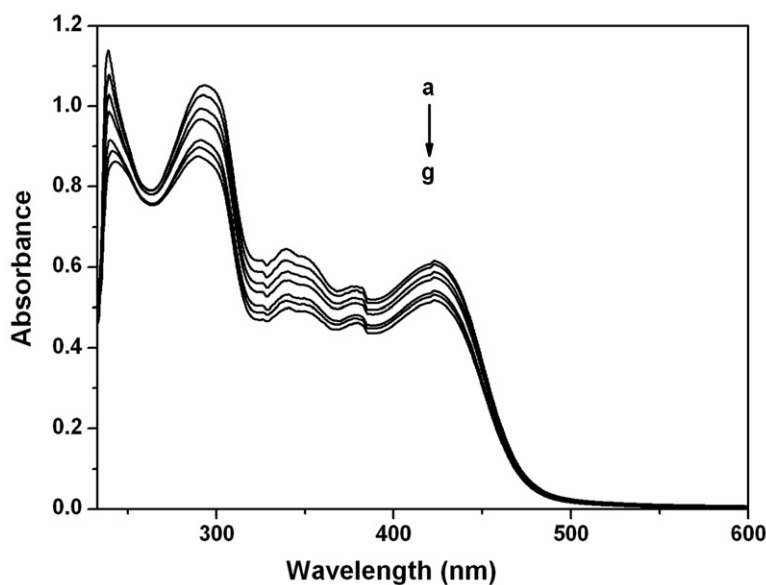


Figure 2. Electronic absorption spectra of $5.0 \times 10^{-5} \text{ mol L}^{-1}$ $[\text{Ni}(\text{QTS})_2] \cdot \text{Cl} \cdot \text{CH}_3\text{OH}$ in the absence (a) and presence (b \rightarrow g) of increasing amounts of CT-DNA at the ratio $r = 0, 0.2, 0.4, 0.6, 0.8, 1.0, 1.2$.

hypochromism (22.4% and 23.8% at 238 and 293 nm, respectively) but no apparent bathochromism were observed, suggesting interactions between DNA and the nickel(II) complex *via* a non-classical intercalation, such as groove binding. Complexes binding with DNA through intercalation result in distinct hypochromism and some bathochromism [50, 51]. The intrinsic binding constant (K_b) obtained for the nickel(II) complex is $3.27 \times 10^3 (\text{mol L}^{-1})^{-1}$ using the absorption at 293 nm, lower than that of classical intercalator EB whose binding constant has been found to be in the order of $10^6 (\text{mol L}^{-1})^{-1}$ [52]. These results suggest that the nickel(II) complex has weaker binding of DNA than the classical intercalator, and it is likely that the nickel(II) complex binds to CT-DNA *via* groove binding.

3.2.2. CD spectra. CD spectra are useful in monitoring the conformational variations of DNA in solution. The CD spectrum of free helix DNA exhibits a positive band at 275 nm due to base stacking and a negative band at 245 nm due to the helicity of B-type DNA [53]. Figure 3 displays the CD spectra of CT-DNA in the absence and presence of $[\text{Ni}(\text{QTS})_2] \cdot \text{Cl} \cdot \text{CH}_3\text{OH}$. The intensities of both the positive and negative bands decrease significantly upon addition of the complex to DNA, which implies that the nickel(II) complex can unwind the DNA helix and lead to the loss of helicity [54, 55]. These changes are indicative of a non-intercalative binding mode and support the groove binding nature [56, 57]; intercalative DNA-binding generally results in an increase of the intensities of both the positive and negative bands in CD spectra.

3.2.3. Fluorescence spectra. Fluorescence spectra were also used to study the interaction between $[\text{Ni}(\text{QTS})_2] \cdot \text{Cl} \cdot \text{CH}_3\text{OH}$ and DNA by measuring the emission

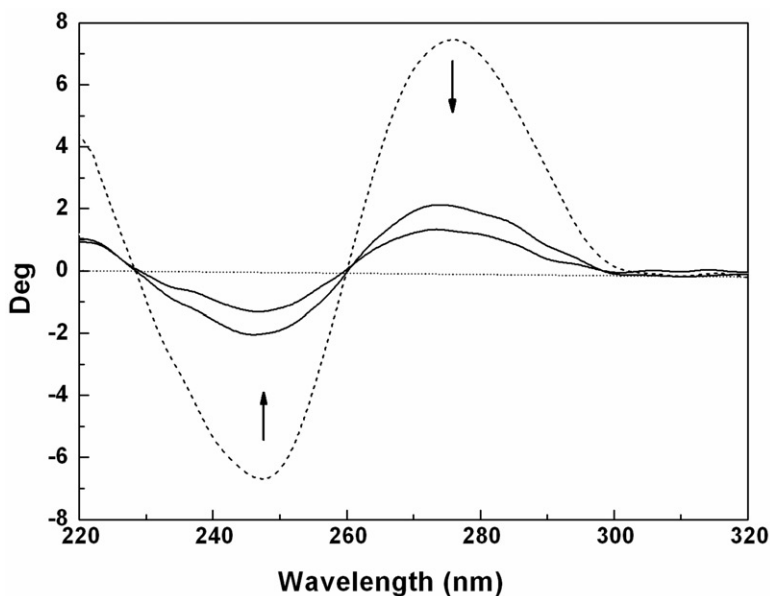


Figure 3. CD spectra of $1.0 \times 10^{-4} \text{ mol L}^{-1}$ CT-DNA in the absence (\cdots) and presence ($-$) of increasing amounts of $[\text{Ni}(\text{QTS})_2] \cdot \text{Cl} \cdot \text{CH}_3\text{OH}$ at the ratio $r = 0, 0.076, 0.13$.

intensity of EB bound to CT-DNA. EB is weakly fluorescent, but can emit intense fluorescence in the presence of DNA because of its intercalative binding to DNA. However, this enhanced fluorescence could be quenched or partly quenched by addition of a second molecule that can replace bound EB or break the secondary structure of DNA [58]. So EB can be used as a probe for determination of DNA structure. In this study, the emission spectra of EB bound to DNA in the absence and presence of $[\text{Ni}(\text{QTS})_2] \cdot \text{Cl} \cdot \text{CH}_3\text{OH}$ are shown in figure 4. The emission intensity of the CT-DNA-EB system ($\lambda_{\text{em}} = 599 \text{ nm}$) decreases with addition of the nickel(II) complex, indicating that the complex can bind to DNA and replace EB from the DNA structure. This behavior suggests that groove binding interactions would occur between the complex and DNA [59, 60], and the electronic absorption spectra and CD spectral analysis also exclude intercalation.

3.3. DNA-cleavage activity

Many nickel(II) complexes that show efficient metallonuclease activity by oxidative or hydrolytic pathways have been reported recently [61–64]. We also studied here the DNA-cleavage activity of $[\text{Ni}(\text{QTS})_2] \cdot \text{Cl} \cdot \text{CH}_3\text{OH}$ by gel electrophoresis using plasmid pBR322 DNA. Figure 5 shows the cleavage of DNA at different concentration of the nickel(II) complex for 1 h reaction time (pH 7.4, 310 K). Control experiments using only ascorbate (H_2A) or nickel(II) complex failed to show apparent cleavage of DNA (figure 5, lanes 2 and 3). With increasing concentration of the nickel(II) complex, the supercoiled DNA (Form I) decreased gradually and was finally converted almost completely to nicked DNA (Form II) in the presence of ascorbate as a reductant agent.

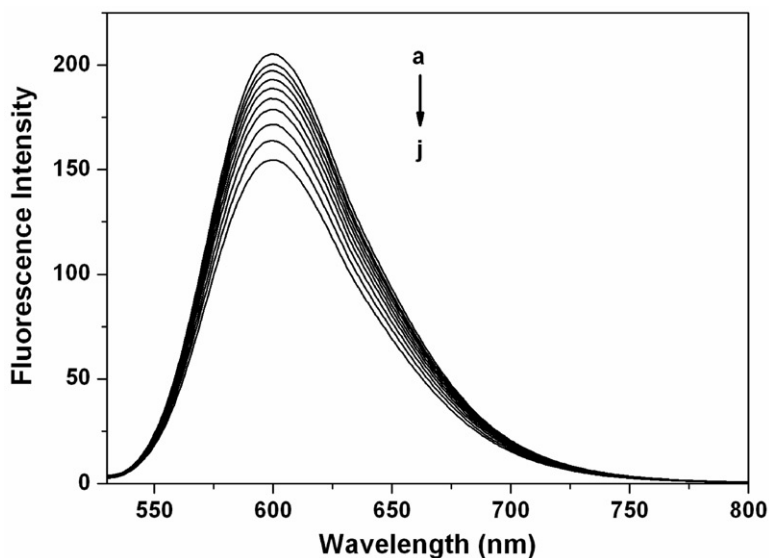


Figure 4. Fluorescence emission spectra (excited at 520 nm) of the CT-DNA-EB system ($1.0 \times 10^{-5} \text{ mol L}^{-1}$ EB, $1.0 \times 10^{-4} \text{ mol L}^{-1}$ CT-DNA) in the absence (a) and presence (b \rightarrow j) of $5.0 \times 10^{-5} \text{ mol L}^{-1}$ $[\text{Ni}(\text{QTS})_2] \cdot \text{Cl} \cdot \text{CH}_3\text{OH}$ ($20 \mu\text{L}$ per scan).

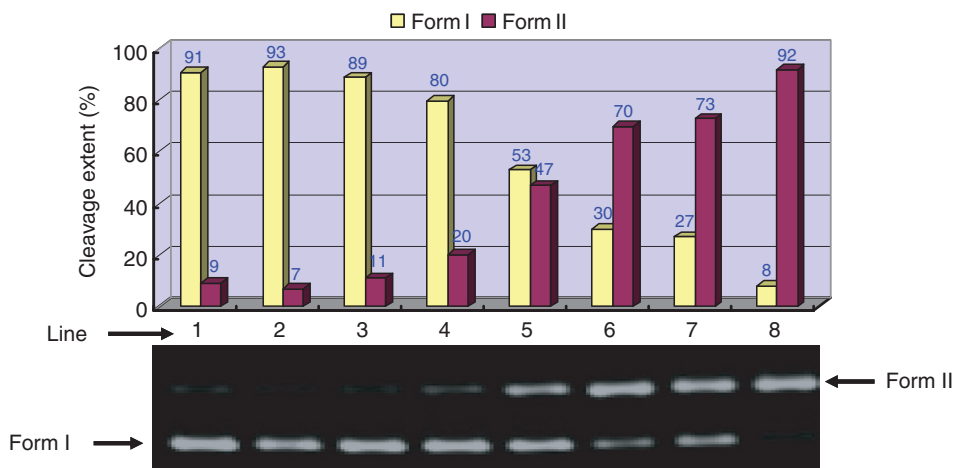


Figure 5. Cleavage of supercoiled pBR322 DNA by $[\text{Ni}(\text{QTS})_2] \cdot \text{Cl} \cdot \text{CH}_3\text{OH}$ at different concentrations in the presence of ascorbate (H_2A) in 5 mmol L^{-1} Tris-HCl/ 50 mmol L^{-1} NaCl buffer (pH 7.4) at 310 K. Lane 1, DNA control; lane 2, DNA + H_2A ; lane 3, DNA + $[\text{Ni}(\text{QTS})_2] \cdot \text{Cl} \cdot \text{CH}_3\text{OH}$ ($10 \mu\text{mol L}^{-1}$); lanes 4–8 represent the DNA-cleavage status at 2, 6, 10, 16, and $24 \mu\text{mol L}^{-1}$ of $[\text{Ni}(\text{QTS})_2] \cdot \text{Cl} \cdot \text{CH}_3\text{OH}$ in the presence of 50-fold excess of H_2A , respectively.

At $24 \mu\text{mol L}^{-1}$, the nickel(II) complex was able to convert 92% of Form I to Form II, which indicated that the nickel(II) complex was efficient in promoting cleavage of plasmid DNA *via* oxidative pathway under the present experimental conditions.

The preliminary mechanism of pBR322 DNA cleavage by $[\text{Ni}(\text{QTS})_2] \cdot \text{Cl} \cdot \text{CH}_3\text{OH}$ was also studied using inhibiting reagents, such as DMSO, *tert*-butyl alcohol, and

histidine (figure 6). It was obviously that the hydroxyl radical scavenger DMSO and *tert*-butyl alcohol diminished the DNA-cleavage activity of the nickel(II) complex, and the singlet oxygen scavenger histidine failed to inhibit cleavage, which indicated that the hydroxyl radical was involved in this cleavage process.

3.4. Cytotoxicity assay

The *in vitro* cytotoxicity of $[\text{Ni}(\text{QTS})_2] \cdot \text{Cl} \cdot \text{CH}_3\text{OH}$ against the human breast cancer cell line MCF-7 and the human non-small-cell lung cancer cell line A-549 were tested using cisplatin as a positive control. The results shown in figure 7 indicate that the nickel(II) complex was more potent against MCF-7 cell line than cisplatin at all

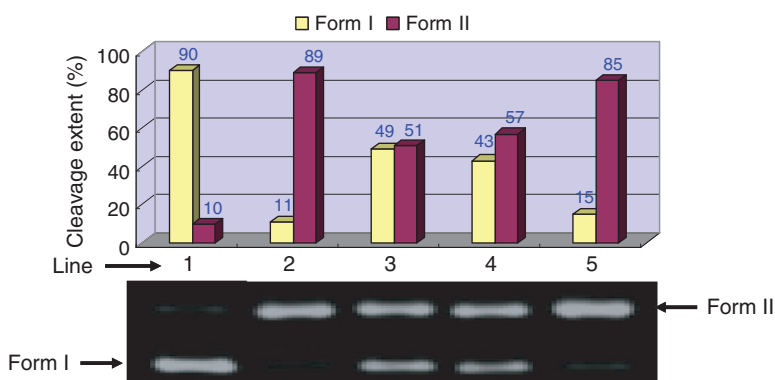


Figure 6. Cleavage of supercoiled pBR322 DNA by $[\text{Ni}(\text{QTS})_2] \cdot \text{Cl} \cdot \text{CH}_3\text{OH}$ ($24 \mu\text{mol L}^{-1}$) in the presence of inhibiting reagents in 5 mmol L^{-1} Tris-HCl/ 50 mmol L^{-1} NaCl buffer (pH 7.4) at 310 K. Lane 1, DNA control; lane 2, DNA + H_2A + $[\text{Ni}(\text{QTS})_2] \cdot \text{Cl} \cdot \text{CH}_3\text{OH}$ ($24 \mu\text{mol L}^{-1}$); lane 3, DNA + H_2A + $[\text{Ni}(\text{QTS})_2] \cdot \text{Cl} \cdot \text{CH}_3\text{OH}$ ($24 \mu\text{mol L}^{-1}$) + DMSO; lane 4, DNA + H_2A + $[\text{Ni}(\text{QTS})_2] \cdot \text{Cl} \cdot \text{CH}_3\text{OH}$ ($24 \mu\text{mol L}^{-1}$) + *t*-butyl alcohol; lane 5, DNA + H_2A + $[\text{Ni}(\text{QTS})_2] \cdot \text{Cl} \cdot \text{CH}_3\text{OH}$ ($24 \mu\text{mol L}^{-1}$) + histidine.

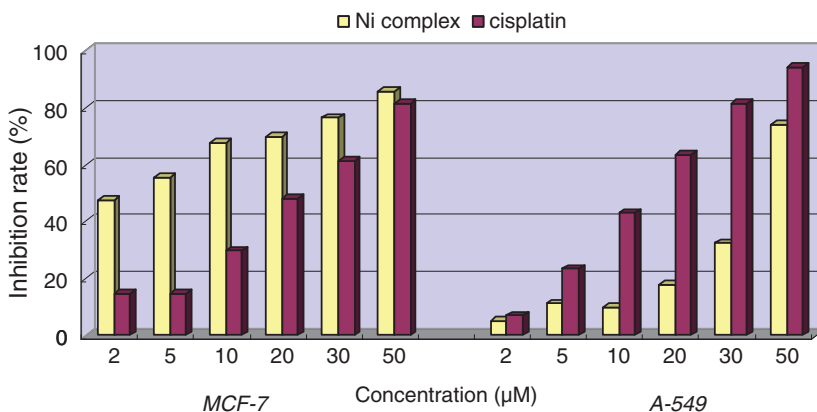


Figure 7. Cytotoxic activity of $[\text{Ni}(\text{QTS})_2] \cdot \text{Cl} \cdot \text{CH}_3\text{OH}$ against the human breast cancer cell line MCF-7 and the human non-small-cell lung cancer cell line A-549 with cisplatin as a positive control.

concentrations tested ($2 \sim 50 \mu\text{mol L}^{-1}$). For example, the inhibition rates of the nickel complex were 47.4% and 55.7% against MCF-7 cell line at the concentration of 2 and $5 \mu\text{mol L}^{-1}$, and were about three to four times higher than that of cisplatin at the same concentration. At a compound concentration of $10 \mu\text{mol L}^{-1}$, the inhibition rate of the nickel complex reached 67.8% against MCF-7 cell line, while the inhibition rate of cisplatin was still only 29.8%. The maximum cell growth inhibition of the nickel complex was similar to that of cisplatin (85.9% and 81.7%, respectively) at $50 \mu\text{mol L}^{-1}$. The nickel complex showed lower cytotoxicity against A-549 cell line compared with cisplatin and is only active with the inhibition rate of 74.1% at concentration of $50 \mu\text{mol L}^{-1}$.

4. Conclusion

We have synthesized and structurally characterized a new nickel(II) complex with thiosemicarbazone of quinoline-2-carboxaldehyde. The complex crystallized in a monoclinic system and nickel(II) has a distorted octahedral geometry. The nickel(II) complex binds with DNA through groove mode and exhibits efficient oxidative DNA cleavage in the presence of ascorbate as reductant. The involvement of hydroxyl radical in the cleavage process was evidenced from inhibition in the presence of DMSO and *tert*-butyl alcohol. *In vitro* cytotoxicity assays demonstrated that the nickel complex was much more active than cisplatin against MCF-7 cell line, which implied that this new nickel(II) complex may have potential as a new antitumor agent.

Supplementary material

Crystallographic data of $[\text{Ni}(\text{QTS})_2] \cdot \text{Cl} \cdot \text{CH}_3\text{OH}$ have been deposited at the Cambridge Crystallographic Data Centre with CCDC No. 854025. Copies of this information may be obtained free of charge from The Director, CCDC, 12 Union Road, Cambridge CB2 1EZ, UK (Fax: +44-1223-336033; E-mail: deposit@ccdc.cam.ac.uk or <http://www.ccdc.cam.ac.uk>).

Acknowledgments

Prof. Guo Zijian (Nanjing University) and Prof. Tan Lifeng (Xiangtan University) are gratefully acknowledged for providing the laboratory facilities. Dr Wang Xiaoyong is gratefully acknowledged for the technical assistance and helpful suggestions.

References

- [1] H. Beraldo, D. Gambino. *Mini Rev. Med. Chem.*, **4**, 31 (2004).
- [2] D.C. Quenelle, K.A. Keith, E.R. Kern. *Antiviral. Res.*, **71**, 24 (2006).

- [3] M. Whitnall, J. Howard, P. Ponka, D.R. Richardson. *Proc. Natl Acad. Sci. USA*, **103**, 14901 (2006).
- [4] D.S. Kalinowski, Y. Yu, P.C. Sharpe, M. Islam, Y.T. Liao, D.B. Lovejoy, N. Kumar, P.V. Bernhardt, D.R. Richardson. *J. Med. Chem.*, **50**, 3716 (2007).
- [5] V. Opletalova, D.S. Kalinowski, M. Vejsová, J. Kuneš, M. Pour, J. Jampilek, V. Buchta, D.R. Richardson. *Chem. Res. Toxicol.*, **21**, 1878 (2008).
- [6] K. Hu, Z.H. Yang, S.S. Pan, H.J. Xu, J. Ren. *Eur. J. Med. Chem.*, **45**, 3453 (2010).
- [7] A.E. Liberta, D.X. West. *BioMetals*, **5**, 121 (1992).
- [8] D. Kovala-Demertzi, M.A. Demertzis, J.R. Miller, C. Papadopoulou, C. Dodorou, G. Filousis. *J. Inorg. Biochem.*, **86**, 555 (2001).
- [9] R.F.F. Costa, A.P. Rebolledo, T. Matencio, H.D.R. Calado, J.D. Ardisson, M.E. Cortés, B.L. Rodrigues, H. Beraldo. *J. Coord. Chem.*, **58**, 1307 (2005).
- [10] D. Kovala-Demertzi, A. Alexandratos, A. Papageorgiou, P.N. Yadav, P. Dalezis, M.A. Demertzis. *Polyhedron*, **27**, 2731 (2008).
- [11] A.E. Graminha, C. Rodrigues, A.A. Batista, L.R. Teixeira, E.S. Fagundes, H. Beraldo. *Spectrochim. Acta, Part A*, **69**, 1073 (2008).
- [12] G. Pelosi, F. Bisceglie, F. Bignami, P. Ronzi, P. Schiavone, M. Carla Re, C. Casoli, E. Pilotti. *J. Med. Chem.*, **53**, 8765 (2010).
- [13] D. Bahl, F. Athar, M.B.P. Soares, M. Santos de Sá, D.R.M. Moreira, R.M. Srivastava, A.C.L. Leite, A. Azam. *Bioorg. Med. Chem.*, **18**, 6857 (2010).
- [14] A.G. Quiroga, C.N. Ranninger. *Coord. Chem. Rev.*, **248**, 119 (2004).
- [15] P. Genova, T. Varadinova, A.I. Matesanz, D. Marinova, P. Souza. *Toxicol. Appl. Pharmacol.*, **197**, 107 (2004).
- [16] B. Wang, Z. Yang, M. Lü, J. Hai, Q. Wang, Z. Chen. *J. Organomet. Chem.*, **694**, 4069 (2009).
- [17] S.A. Khan, M. Yusuf. *Eur. J. Med. Chem.*, **44**, 2270 (2009).
- [18] D.L. Klayman, J.F. Bartosevich, T.S. Griffin, C.J. Mason, J.P. Scovill. *J. Med. Chem.*, **22**, 855 (1979).
- [19] J. Li, L.M. Zheng, I. King, T.W. Doyle, S.H. Chen. *Curr. Med. Chem.*, **8**, 121 (2001).
- [20] D.R. Richardson, P.C. Sharpe, D.B. Lovejoy, D. Senaratne, D.S. Kalinowski, M. Islam, P.V. Bernhardt. *J. Med. Chem.*, **49**, 6510 (2006).
- [21] D.R. Richardson, D.S. Kalinowski, V. Richardson, P.C. Sharpe, D.B. Lovejoy, M. Islam, P.V. Bernhardt. *J. Med. Chem.*, **52**, 1459 (2009).
- [22] H. Huang, W. Chen, X. Ku, L. Meng, L. Lin, X. Wang, C. Zhu, Y. Wang, Z. Chen, M. Li, H. Jiang, K. Chen, J. Ding, H. Liu. *J. Med. Chem.*, **53**, 3048 (2010).
- [23] R.W. Brockman, J.R. Thomson, M.J. Bell, H.E. Skipper. *Cancer Res.*, **16**, 167 (1956).
- [24] R.C. DeConti, B.R. Toftness, K.C. Agrawal, R. Tomchick, J.A.R. Mead, J.R. Bertino, A.C. Sartorelli, W.A. Creasey. *Cancer Res.*, **32**, 1455 (1972).
- [25] I.H. Krakoff, E. Etcubanas, C. Tan, K. Mayer, V. Bethune, J.H. Burchenal. *Cancer Chemother. Rep.*, **58**, 207 (1974).
- [26] M.J. Mackenzie, D. Saltman, H. Hirte, J. Low, C. Johnson, G. Pond, M.J. Moore. *Invest. New Drugs*, **25**, 553 (2007).
- [27] J.E. Karp, F.J. Giles, I. Gojo, L. Morris, J. Greer, B. Johnson, M. Thein, M. Sznol, J. Low. *Leuk. Res.*, **32**, 71 (2008).
- [28] B. Ma, B.C. Goh, E.H. Tan, K.C. Lam, R. Soo, S.S. Leong, L.Z. Wang, F. Mo, A.T.C. Chan, B. Zee, T. Mok. *Invest. New Drugs*, **26**, 169 (2008).
- [29] M.C. Miller, C.N. Stineman, J.R. Vance, D.X. West, I.H. Hall. *Anticancer Res.*, **18**, 4131 (1998).
- [30] S. Adsule, V. Barve, D. Chen, F. Ahmed, Q.P. Dou, S. Padhye, F.H. Sarkar. *J. Med. Chem.*, **49**, 7242 (2006).
- [31] C.R. Kowol, R. Trondl, P. Heffeter, V.B. Arion, M.A. Jakupec, A. Roller, M. Galanski, W. Berger, B.K. Keppler. *J. Med. Chem.*, **52**, 5032 (2009).
- [32] B.M. Zeglis, V. Divilov, J.S. Lewis. *J. Med. Chem.*, **54**, 2391 (2011).
- [33] M.J. Waring. *Ann. Rev. Biochem.*, **50**, 159 (1981).
- [34] S.J. Berners-Price, P.J. Sadler. *Coord. Chem. Rev.*, **151**, 1 (1996).
- [35] Z.J. Guo, P.J. Sadler. *Adv. Inorg. Chem.*, **49**, 183 (2000).
- [36] G.M. Sheldrick. *SHELXTL v5, Reference Manual, Siemens Analytical X-ray Systems*, Madison, WI (1996).
- [37] J. Marmur. *J. Mol. Biol.*, **3**, 208 (1961).
- [38] M.E. Reichmann, S.A. Rice, C.A. Thomas, P. Doty. *J. Am. Chem. Soc.*, **76**, 3047 (1954).
- [39] A. Wolfe, G.H. Shimer, T. Meehan. *Biochemistry*, **26**, 6392 (1987).
- [40] M.C. Alley, D.A. Scudiero, A. Monks, M.L. Hursey, M.J. Czerwinski, D.L. Fine, B.J. Abbott, J.G. Mayo, R.H. Shoemaker, M.R. Boyd. *Cancer Res.*, **48**, 589 (1988).
- [41] P. Skehan, R. Storeng, D. Scudiero, A. Monks, J. McMahon, D. Vistica, J.T. Warren, H. Bokesch, S. Kenney, M.R. Boyd. *J. Natl Cancer Inst.*, **82**, 1107 (1990).
- [42] S.C. Zhang, C. Tu, X.Y. Wang, Z.Y. Yang, J.Y. Zhang, L.P. Lin, J. Ding, Z.J. Guo. *Eur. J. Inorg. Chem.*, 4028 (2004).
- [43] M.A. Ali, A.H. Mirza, F.H. Bujang, M.H.S.A. Hamid, P.V. Bernhardt. *Polyhedron*, **25**, 3245 (2006).

- [44] R. Gil-García, R. Zichner, V. Díez-Gómez, B. Donnadiou, G. Madariaga, M. Insausti, L. Lezama, P. Vitoria, M.R. Pedrosa, J. García-Tojal. *Eur. J. Inorg. Chem.*, 4513 (2010).
- [45] M.A. Ali, S.M.M.H. Majumder, R.J. Butcher, J.P. Jasinski, J.M. Jasinski. *Polyhedron*, **16**, 2749 (1997).
- [46] M. Mathew, G.J. Palenik. *J. Am. Chem. Soc.*, **91**, 6300 (1969).
- [47] A.F. Taniou, D.Y. Ding, D.A. Patrick, C. Bailly, R.R. Tidwell, W.D. Wilson. *Biochemistry*, **39**, 12091 (2002).
- [48] E.W. Ainscough, E.N. Baker, A.M. Brodie, R.J. Cresswell, J.D. Ranford, J.M. Waters. *Inorg. Chim. Acta*, **172**, 185 (1990).
- [49] T.B.S.A. Ravoo, K.A. Crouse, M.I.M. Tahir, A.R. Cowley, M.A. Ali. *Polyhedron*, **26**, 1159 (2007).
- [50] J.K. Barton, A.T. Danishefsky, J.M. Goldberg. *J. Am. Chem. Soc.*, **106**, 2172 (1984).
- [51] R.B. Nair, E.S. Tang, S.L. Kirkland, C.J. Murphy. *Inorg. Chem.*, **37**, 139 (1998).
- [52] M.J. Waring. *J. Mol. Biol.*, **13**, 269 (1965).
- [53] A. Rajendran, B.U. Nair. *Biochim. Biophys. Acta*, **1760**, 1794 (2006).
- [54] R.F. Pasternack. *Chirality*, **15**, 329 (2003).
- [55] K. Karidi, A. Garoufis, N. Hadjiliadis, J. Reedijk. *Dalton Trans.*, 728 (2005).
- [56] P.U. Maheswari, M. Palaniandavar. *J. Inorg. Biochem.*, **98**, 219 (2004).
- [57] P.X. Xi, Z.H. Xu, F.J. Chen, Z.Z. Zeng, X.W. Zhang. *J. Inorg. Biochem.*, **103**, 210 (2009).
- [58] Y.F. Song, P. Yang. *Polyhedron*, **20**, 501 (2001).
- [59] B.C. Baguley. *Mol. Cell. Biochem.*, **43**, 167 (1982).
- [60] A.G. Krishna, D.V. Kumar, B.M. Khan, S.K. Rawal, K.N. Ganesh. *Biochim. Biophys. Acta*, **1381**, 104 (1998).
- [61] L.N. Zhu, D.M. Kong, X.Z. Li, G.Y. Wang, J. Wang, Y.W. Jin. *Polyhedron*, **29**, 574 (2010).
- [62] J. Xu, Y.F. Chen, H. Zhou, Z.Q. Pan. *J. Coord. Chem.*, **64**, 1626 (2011).
- [63] Q.R. Cheng, J.Z. Chen, H. Zhou, Z.Q. Pan. *J. Coord. Chem.*, **64**, 1139 (2011).
- [64] J.C. Joyner, J. Reichfield, J.A. Cowan. *J. Am. Chem. Soc.*, **133**, 15613 (2011).